

---

# Nonlinear Absorption and Refractive Index of Raman Scattered Mode in Magnetized Diffusive Semiconductor Plasmas

Ritu Chaudhary

Department of Physics, Singhania University, Pachari Bari, Jhunjhunu, India

Manjeet Singh

Ex. Assistant Prof., Department of Physics, Amity University, Noida-201301, India

## ABSTRACT

Using hydrodynamic model of a semiconductor plasma, a detailed analytical investigation is made of the Raman instability of Stokes component of scattered wave in an obliquely magnetized (with respect to the direction of propagation) centrosymmetric semiconductor. The origin of stimulated Raman scattering process lies in effective third-order optical susceptibility  $\chi_{eff}^{(3)}$  arising due to induced nonlinear current density and the interaction of pump wave with the density fluctuations generated within the medium. The total refractive index and absorption coefficient are determined via  $\chi_{eff}^{(3)}$ . The threshold pump intensity and optimum pulse duration for Raman gain are obtained. The analysis establishes that large refractive index and small absorption coefficient can be obtained in a magnetized diffusive semiconductor plasma which proves its potential as candidate material for fabrication of cubic nonlinear devices.

## Keywords

Nonlinear phenomena, wave interactions, refractive index, absorption coefficient, optical susceptibility, III-V semiconductors.

## INTRODUCTION

Stimulated scattering of laser radiation is one of the most active areas of research in the field of nonlinear optics, on one hand, it provides fundamental and microscopic information of the interaction of laser beam with matter, and on the other hand it has numerous applications in the area of modern optics [1]. When an intense laser beam propagates in a medium, it may excite the natural mode of vibrations of the medium, i.e., the electron-plasma and ion waves. When one of the excited modes is of high frequency, it gives rise to stimulated Raman scattering (SRS) [2, 3]. SRS is among the earliest-discovered nonlinear optical processes. In SRS process, the pump decays into another electromagnetic wave and a Langmuir wave. Such a phenomenon was first observed by Woodburg and Ng [4] in organic and inorganic liquids. An analysis of the scattered radiation reveals the existence of frequencies that are shifted down or up by increments equal to vibrational frequencies of the material irradiated and are referred to as Stokes and anti-Stokes scattering, respectively. The theoretical description of SRS was given by Hellwarth [5], who treated it as a two-photon process with full quantum mechanical calculations.

Various aspects of SRS and its consequent instabilities have been investigated in gaseous plasmas [6-8]. But the practical utilization of semiconductors drew the attention of many solid-state physicists to examine the role of semiconductors in the areas such as spectroscopy, lasers, device fabrication etc. The electrical properties of semiconductors lie in between those of metals with nearly free electrons and insulators with tightly bound electrons. This intermediate situation makes semiconductors attractive as nonlinear devices in electronics as well optics because their properties can be influenced easily by fields, compositions and micro-structuring. Hence, the supremacy of semiconductors as active media in laser communication, modern optoelectronic devices, optical computing [9] and all optical signal processing [10] is unquestionable and

hence the understanding of the mechanisms of transient effects in these crystals appears to be of fundamental significance.

In the recent past, a significant amount of research work on SRS and its consequent instabilities in magnetized centrosymmetric as well as non-centrosymmetric semiconductor plasmas have been reported by several groups [11-15]; the theoretical predictions and experimental measurements are far apart. Several experiments, with short laser pulses of low intensity, suggest that SRS starts below the theoretically estimated threshold value, whereas some experiments with high-intensity radiation reveal that SRS signal levels saturate at much lower values than their theoretically predicted values. Hence, more comprehensive efforts in SRS theory are needed.

In most of the investigations of nonlinear interactions the nonlocal effects such as diffusion of the excitation density that is responsible for the nonlinear refractive index change has been ignored. The diffusion of carriers is however expected to have strong influence on the nonlinearity of the medium, particularly in high mobility semiconductors viz., III-V compound semiconductors. Therefore inclusion of carrier diffusion in theoretical studies of nonlinear phenomenon seems to be important from both the fundamental and applied view points, and has thus attracted the attention of many groups recently [16-20].

Apart from material parameters, the optical properties of a material can be modified by an externally applied electric or magnetic field. The refractive index and absorption coefficient as functions of the applied electric and magnetic fields are responsible for many electro-optical and magneto-optical effects. Thus recent attention has focused on the theoretical and experimental investigations of stimulated emission and resonant amplification of far-infrared radiation in the presence of the electric and magnetic fields. In the presence of a static magnetic field, the medium supports many new modes and offers many new channels for scattering. Several groups [11-15] have studied SRS of a plane polarized pump wave in magnetized crystals. Their case corresponds to the propagation of a pump wave exactly either parallel or perpendicular to the external static magnetic field. Such an exact parallel or perpendicular propagation may not be experimentally feasible. Moreover the electric field of the pump considered by them is parallel to the propagation vector. This again is not the case of realistic situation. For a finite semiconductor plasma pump electric field  $\vec{E}_0$  must have components that are both parallel and perpendicular to propagation direction. Thus the most realistic case is to consider a hybrid mode propagating obliquely to the external magnetic field.

However, as far as the authors know, no such attempt has been made to determine the third-order optical susceptibility arising due to the diffusion induced current density and molecular vibrations and subsequently the nonlinear refractive index and effective absorption coefficient. In the present paper, the authors have investigated analytically the nonlinear absorption coefficient and refractive index arising due to the SRS of an electromagnetic hybrid wave propagating obliquely in magnetized diffusive semiconductor plasma. The physical origin of the process lies in the non-vanishing, nonlinear polarization due to the coupling of the molecular vibrations having a frequency equal to that of the optical phonon frequency  $\omega_{op}$  with the pump frequency  $\omega_0$ , as well as the electron plasma frequency  $\omega_p$  in the presence of a static magnetic field such that  $\omega_{op} < \omega_p < \omega_0$ . The motivation for the present investigation stems from the fact that the diffusion of excess carriers can remarkably modify the nonlinearity of medium. In the wake of high power lasers, such an investigation with high mobility semiconductor plasmas becomes even more important because it may lead to a better understanding of the scattering mechanisms in plasma and thus may prove to be a step forward towards filling the gap between theory and experimental observations.

## THEORETICAL FORMULATIONS

This section deals with the theoretical formulation of the total-induced current density  $\mathbf{J}$  for the signal and the Stoke's component of the scattered electromagnetic wave in magnetized diffusive semiconductor plasma. The well-known hydrodynamic model of a homogeneous n-type semiconductor-plasma with electrons as carriers

subjected to an electromagnetic pump field under thermal equilibrium is considered. In order to study the total-induced current density  $\mathbf{J}$ , let us consider the propagation of a hybrid pump wave

$$\mathbf{E}_0 = (E_{0x}\hat{i} + E_{0y}\hat{j})\exp[i(k_0x - \omega_0t)] \quad (1)$$

in a homogeneous n-type III-V diffusive semiconductor viz. n-InSb embed in a uniform static magnetic field  $\mathbf{B}_0 = B_{0x}\hat{i} + B_{0z}\hat{k}$  in a direction making an angle  $\theta$  with the  $x$ -axis, as shown in Fig. 1.

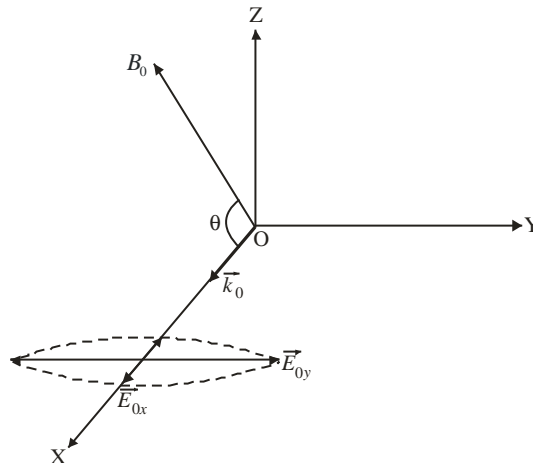


**Fig. 1. Geometry of SRS in magnetic field.**

In a Raman active medium the scattering of high frequency pump wave is enhanced due to excitation of a normal vibrational mode. Let us consider that the Raman medium consists of  $N$  harmonic oscillators per unit volume; each oscillator being characterized by its position  $x$  and normal vibrational coordinates  $u(x, t)$ . The Eq. of motion of a single oscillator (optical phonon) is then represented as:

$$\frac{\partial^2 u(x, t)}{\partial t^2} + \Gamma_{op} \frac{\partial u(x, t)}{\partial t} + \omega_{op}^2 u(x, t) = \frac{F(x, t)}{M}, \quad (2)$$

where,  $\Gamma_{op}$  is the damping constant equal to the phenomenological phonon-collision frequency ( $\sim 10^{-2}\omega_i$ );  $\omega_{op}$  being the un-damped molecular vibrational frequency and is taken to be equal to the transverse optical phonon frequency and  $M$  is the mass.  $F(x, t)$  is the driving force per unit volume, which can be obtained by considering the electromagnetic energy in polarizable materials and is given by

$$F(x, t) = \frac{1}{2} \varepsilon \left( \frac{\partial \alpha}{\partial u} \right)_0 [\mathbf{E}_{eff} \cdot \mathbf{E}_1^*]. \quad (3)$$

Here  $\varepsilon = \varepsilon_0 \varepsilon_\infty$ ;  $\nu_0$  and  $\nu_\infty$  are the absolute and high frequencies permittivities, respectively.  $(\partial \alpha / \partial u)_0$  represents the differential polarizability.  $\mathbf{E}_{eff} = \mathbf{E}_0 + (\mathbf{v}_0 \times \mathbf{B}_0)$  represents the effective electric field which includes the Lorentz force  $(\mathbf{v}_0 \times \mathbf{B}_0)$  in the presence of external static magnetic field  $\mathbf{B}_0$ .  $\mathbf{E}_1$  is the space charge electric field. This infers that natural mode of vibrations within the medium can be driven by the optical electric field because of non-vanishing polarizability  $(\partial \alpha / \partial u)_0$ .

The other basic Eq.s of the analysis are:

$$\frac{\partial \mathbf{v}_0}{\partial t} + \nu \mathbf{v}_0 + \left( \mathbf{v}_0 \cdot \frac{\partial}{\partial x} \right) \mathbf{v}_0 = -\frac{e}{m} \mathbf{E}_{eff} \quad (4)$$

$$\frac{\partial \mathbf{v}_1}{\partial t} + \mathbf{v} \mathbf{v}_1 + \left( \mathbf{v}_0 \cdot \frac{\partial}{\partial x} \right) \mathbf{v}_1 + \left( \mathbf{v}_1 \cdot \frac{\partial}{\partial x} \right) \mathbf{v}_0 = -\frac{e}{m} [\mathbf{E}_1 + \mathbf{v}_1 \times \mathbf{B}_0] \quad (5)$$

$$\mathbf{P}_{mv} = \epsilon N \left( \frac{\partial \alpha}{\partial u} \right)_0 u^* \mathbf{E}_{eff} \quad (6)$$

$$\frac{\partial n_1}{\partial t} + v_0 \frac{\partial n_1}{\partial x} + n_0 \frac{\partial v_1}{\partial x} + D \frac{\partial^2 n_1}{\partial x^2} = 0 \quad (7)$$

$$\frac{\partial E_1}{\partial x} = -\frac{n_1 e}{\epsilon} - N \left( \frac{\partial \alpha}{\partial u} \right)_0 \frac{\partial u^*}{\partial x} E_0 \quad (8)$$

Eqs. (4) and (5) represent the rate Eqs for the pump and the signal beam under the influence of a static magnetic field, respectively.  $\mathbf{v}_0$  and  $\mathbf{v}_1$  are the equilibrium and perturbed oscillatory fluid velocities of the electrons of effective mass  $m$  and charge  $e$ . Here  $\mathbf{v}$  the momentum-transfer collision frequency of electrons.  $\mathbf{P}_{mv}$  given by Eq. (6) is the nonlinear polarization due to modulation of dielectric constant of the medium and natural mode of vibrations driven by the electric field. At very high frequencies of the field, which are quite large as compared to the frequencies of the motion of electrons in the medium, the polarization is determined by neglecting the interactions of the electrons with one another and with nuclei of atoms. Thus the electric displacement in the presence of an external magnetic field is simply given by  $\mathbf{D} = \epsilon \mathbf{E}_{eff}$ . Eq. (7) is the continuity Eq. including diffusion effects, where  $n_0$ ,  $n_1$  and  $D$  are the equilibrium and perturbed electron densities and diffusion coefficient respectively. The strong space-charge  $\mathbf{E}_1$  developed due to migration of charge carriers under the influence of the pump and magnetic fields is determined from Poisson Eq. [Eq. (8)].

The interaction of the pump with the molecular vibrations produces an electron density perturbation, which in turn derives an electron-plasma wave and induces current density in the Raman active medium. In a doped semiconductor, this density perturbation can be obtained by using a method adopted by Singh et.al. [21]. Differentiating Eq. (7) and using Eqs. (4) and (8), we obtain

$$\frac{\partial^2 n_1}{\partial t^2} + v \frac{\partial n_1}{\partial t} + v D \frac{\partial^2 n_1}{\partial x^2} + \left[ \bar{\omega}_p^2 \left( \frac{v^2}{v^2 + \omega_{cz}^2} \right) \right] n_1 + \frac{\epsilon N k_1 \omega_p^2 u^*}{2eM} \left( \frac{\partial \alpha}{\partial u} \right)_0 E_{eff} = \frac{ik_1 n_1 e}{m} E_{eff} \quad (9)$$

where  $\bar{\omega}_p^2 = \omega_p^2 \left( \frac{\omega_{cx}^2 + v^2}{\omega_c^2 + v^2} \right)$ ;  $\omega_{cx,z} \left( = \frac{-eB_{0x,z}}{m} \right)$  are the components of cyclotron frequency along the  $x$ - and  $z$ -axes and  $\omega_p \left[ = \left( \frac{n_0 e^2}{m\epsilon} \right)^{1/2} \right]$  is the plasma frequency of carriers in the medium. The Doppler shift has been neglected under the assumption that  $\omega_0 \gg v \gg k_0 v_0$ .

As per the method adopted by Singh et.al. [21], the perturbed electron density ( $n_1$ ) produced in the medium may be divided into two components; one associated with optical phonon mode ( $n_{1op}$ ) and varies as  $\exp[i(k_{op}x - \omega_{op}t)]$  and other associated with first-order Stokes mode ( $n_{1st}$ ) and varies as  $\exp[i(k_1x - \omega_1t)]$ .

The process of SRS may also be described as the annihilation of a pump photon and simultaneous creation of one scattered photon and one induced photon. Hence, for these modes, the stimulated Raman process under consideration should satisfy the phase matching conditions:  $\hbar\omega_0 = \hbar\omega_1 + \hbar\omega_{op}$  and  $\hbar k_0 = -\hbar k_1 + \hbar k_{op}$  known as the energy and momentum conservation relations which determine the frequency shift and direction of

propagation of scattered light. By assuming a long interaction path for the interacting waves, only the resonant Stokes component ( $\omega_1 = \omega_0 - \omega_a, k_1 = k_0 - k_{op}$ ) are considered, and the off resonant higher-order components are neglected [22]. Here  $(\omega_1, k_1)$  represents the Stoke's modes.

Under rotating-wave-approximation (RWA), perturbed density of Raman active medium associated with optical phonon ( $n_{1op}$ ) and first-order Stokes mode ( $n_{1st}$ ) can be deduced from Eq. (9) as:

$$\frac{\partial^2 n_{1st}}{\partial t^2} + v \frac{\partial n_{1st}}{\partial t} + vD \frac{\partial^2 n_{1st}}{\partial x^2} + \left[ \bar{\omega}_p^2 \left( \frac{v^2}{v^2 + \omega_{cz}^2} \right) \right] n_{1st} + \frac{\varepsilon N k_1 \omega_p^2 u^*}{2eM} \left( \frac{\partial \alpha}{\partial u} \right)_0 E_{eff} = \frac{ik_1 n_{1s}^* e}{m} E_{eff} \quad (10a)$$

and

$$\frac{\partial^2 n_{1op}}{\partial t^2} + v \frac{\partial n_{1op}}{\partial t} + vD \frac{\partial^2 n_{1op}}{\partial x^2} + \left[ \bar{\omega}_p^2 \left( \frac{v^2}{v^2 + \omega_{cz}^2} \right) \right] n_{1op} = -\frac{ik_1 n_{1op}^* e}{m} E_{eff}. \quad (10b)$$

The above Eqs. represent the coupling between optical phonon and first-order Stoke's mode of the density perturbations via effective electric field  $E_{eff}$ , which acts as a distributed source that can feed energy to the scattered Stoke's component leading to the amplification of this field with a large gain coefficient. Hence it is obvious that the presence of the pump field is of fundamental necessity for stimulated Raman scattering to occur. By solving simultaneous Eqs (10a) and (10b),  $n_{1op}$  can be obtained as:

$$n_{1op} = \frac{\varepsilon_0 \varepsilon_\infty \omega_p^2 N k_{op} (\partial \alpha / \partial u)_0^2 E_{eff} E_1^*}{2eM (\delta_{op}^2 - 2i\Gamma_{op} \omega_{op})} \left[ 1 - \frac{(\delta_1^2 - iv\omega_1)(\delta_2^2 + iv\omega_{op})}{k_1^2 (e/m)^2 E_{eff}^2} \right]^{-1}. \quad (11)$$

$$\text{Here } \delta_{op}^2 = \omega_{op}^2 - k_{op}^2 v^2, \delta_1^2 = \bar{\omega}_p^2 \left( \frac{v^2}{v^2 + \omega_{cz}^2} \right) - \omega_1^2 - k^2 vD, \text{ and } \delta_2^2 = \bar{\omega}_p^2 \left( \frac{v^2}{v^2 + \omega_{cz}^2} \right) - \omega_{op}^2 - k^2 vD.$$

It is evident from the above expression that  $n_{1op}$  strongly depends upon the magnitude of the pump intensity. The density perturbation thus produced affects the propagation characteristics of the generated waves.

Now the resonant Stoke's component  $(\omega_1, k_1)$  of the current density due to finite nonlinear polarization of the medium has been deduced by neglecting the transition dipole moment, which can be represented as:

$$\begin{aligned} \mathbf{J}(\omega_1) &= n_0 e v_{1x} + n_{1s}^* e v_{0x} \\ &= -\frac{\bar{\omega}_p^2 v \varepsilon E_1}{(v^2 + \omega_{cz}^2)} - \frac{\varepsilon_0 \bar{\omega}_p^2 N k_{op} (\partial \alpha / \partial u)_0^2 E_{eff}^* E_0 E_1 (v - i\omega_0)}{2eM (\delta_{op}^2 - 2i\Gamma_{op} \omega_{op}) (\omega_{cz}^2 - \omega_0^2)} \left( 1 - \frac{(\delta_1^2 - iv\omega_1)(\delta_2^2 + iv\omega_{op})}{k_1^2 (e/m)^2 E_{eff}^2} \right)^{-1} \\ &= \mathbf{J}_l(\omega_1) + \mathbf{J}_{nl}(\omega_1) \end{aligned} \quad (12)$$

The first term of the above expression [i.e.,  $\mathbf{J}_l(\omega_1)$ ] represents the linear component of the induced current density. The second term [i.e.,  $\mathbf{J}_{nl}(\omega_1)$ ] represents the nonlinear coupling amongst the three interacting waves via the total nonlinear current density including the diffusion current.

Now treating the induced polarization  $\mathbf{P}_{cd}(\omega_1)$  as the time integral of induced current density  $\mathbf{J}(\omega_1)$ , we may write

$$\mathbf{P}_{cd}(\omega_1) = \int \mathbf{J}(\omega_1) dt \quad (13)$$

In order to study the effective optical susceptibility  $\chi_e$ , the induced polarization in a centrosymmetric crystal can be expressed in the form of an expansion series as:

$$\mathbf{P}_{cd}(\omega_1) = \epsilon_0 \chi \mathbf{E}_1(\omega_1) = \epsilon_0 \left[ \chi^{(1)} + \chi^{(2)} |E_{eff}|^2 + \dots \right] \mathbf{E}_1(\omega_1) \quad (14)$$

where  $\chi^{(1)}$  and  $\chi^{(3)}$  are the first- and third-order optical susceptibilities due to the induced current density, respectively. Because of inversion symmetry  $\chi^{(2)}$ ,  $\chi^{(4)}$  etc. are all zero. Using Eqs. (12) and (13), an expression for  $\mathbf{P}_{cd}(\omega_1)$  will be obtained; now equating the expressions corresponding to the same power of  $\mathbf{E}_1(\omega_1)$  in this derived Eq. and Eq. (14), we obtain

$$\chi_{cd}^{(1)} = \frac{i\epsilon_1 \bar{\omega}_p^2}{\omega_1(\omega_0^2 - \omega_{cz}^2)} \quad (15)$$

and

$$\chi_{cd}^{(3)} = \frac{\omega_0^3 \bar{\omega}_p^2 N k_{op} (\partial \alpha / \partial u)_0^2}{2eM \omega_1 (\delta_{op}^2 - 2i\Gamma_{op} \omega_{op})(\omega_0^2 - \omega_{cz}^2)^2} \left( 1 - \frac{(\delta_1^2 - i\nu\omega_1)(\delta_2^2 + i\nu\omega_{op})}{k_1^2 (e/m)^2 E_{eff}^2} \right)^{-1}. \quad (16)$$

Besides the nonlinear induced polarization due to the perturbed current density, the system should also possess a polarization created by the interaction of the pump with the normal mode of vibrations generated within the medium. The scattering of the pump wave from the optical phonons affords a convenient mean of controlling the frequency, intensity and direction of scattered beam. This type of control makes a large number of applications possible involving the transmission, display and processing of information. The molecular polarization is obtained from Eq. (6) as:

$$P_{mv} = \frac{\epsilon_0 \omega_0^4 N k_{op} (\partial \alpha / \partial u)_0^2 |E_{eff}|^2 E_1}{2eM (\delta_{op}^2 - 2i\Gamma_{op} \omega_{op})(\omega_0^2 - \omega_{cz}^2)^2} = \epsilon_0 \chi_{mv}^{(3)} |E_{eff}|^2 E_1. \quad (17)$$

Thus in a doped centrosymmetric crystal the effective third-order optical susceptibility  $\chi_{eff}^{(3)}$  is given by

$$\chi_{eff}^{(3)} = \chi_{cd}^{(3)} + \chi_{mv}^{(3)}. \quad (18)$$

Using Eqs. (16) – (18), we obtain

$$\begin{aligned} \chi_{eff}^{(3)} &= \frac{\omega_0^3 N k_{op} (\partial \alpha / \partial u)_0^2}{2eM (\omega_0^2 - \omega_{cz}^2)^2 (\delta_{op}^2 - 2i\Gamma_{op} \omega_{op})} \left[ \frac{\bar{\omega}_p^2}{\omega_1} \left( 1 - \frac{(\delta_1^2 - i\nu\omega_1)(\delta_2^2 + i\nu\omega_{op})}{k_1^2 (e/m)^2 E_{eff}^2} \right)^{-1} + \omega_0 \right] \\ &= [\chi_{eff}^{(3)}]_{real} + [\chi_{eff}^{(3)}]_{imag}, \end{aligned} \quad (19)$$

in which  $[\chi_{eff}^{(3)}]_{real}$  and  $[\chi_{eff}^{(3)}]_{imag}$  represent the real and imaginary parts of effective third-order (Raman) susceptibility. Here  $k_a = [k_0^2 + k_1^2 - 2k_0 k_1 \cos \phi]^{1/2}$ , where  $\phi$  is the scattering angle between  $\mathbf{k}_1$  and  $\mathbf{k}_0$ .

The total refractive index of the system is given by [23]

$$\eta = \eta_l + \eta_{nl} |E_{eff}|^2, \quad (20)$$

in which  $\eta_l$  and  $\eta_{nl}$  are, respectively, the linear and nonlinear parts of the refractive index of the material. From the real parts of  $\chi^{(1)}$  i.e.,  $[\chi^{(1)}]_{real}$  and  $\chi_{eff}^{(3)}$  i.e.,  $[\chi_{eff}^{(3)}]_{real}$ , we may study the phenomenon of the total refractive index in centrosymmetric crystals because  $\eta_l$  and  $\eta_{nl}$  are given by

$$\eta_l = \sqrt{1 + [\chi_{cd}^{(1)}]_{real}} \quad (21)$$

and

$$\eta_{nl} = [\chi_{eff}^{(3)}]_{real} \quad (22)$$

Now to study the total absorption coefficient  $\alpha$ , one may use the following standard relation

$$\alpha = \alpha_l + \alpha_{nl} |E_{eff}|^2, \quad (23)$$

in which  $\alpha_l$  and  $\alpha_{nl}$  are the linear and nonlinear absorption coefficients. From the imaginary parts of  $\chi^{(1)}$  i.e.,  $[\chi^{(1)}]_{imag}$  and  $\chi_{eff}^{(3)}$  i.e.,  $[\chi_{eff}^{(3)}]_{imag}$ , in the following relations, the phenomenon of total absorption can be studied in the centrosymmetric crystals. These relations are

$$\alpha_l = \sqrt{[\chi^{(1)}]_{imag}} \quad (24)$$

and

$$\alpha_{nl} = -\frac{k_1}{2\varepsilon_1} \sqrt{[\chi_{eff}^{(3)}]_{imag}}. \quad (25)$$

Eqs. (20) and (23) can be employed to study the nonlinear parameters (refractive and absorptive) of a Raman active magnetized diffusive semiconductor plasma.

The steady-state Raman gain coefficient of the Stokes component in the presence of a pump well above the threshold value is obtained as [21]:

$$g_R(\omega_1) = -\frac{\omega_1}{\eta c_0} [\chi_{eff}^{(3)}]_{imag} |E_{eff}|^2, \quad (26)$$

where  $c_0$  being the velocity of light in vacuum.

The transient gain factor  $g_{TR}$  is related to steady-state gain coefficient [24] through

$$g_{TR} = (2g_R x \Gamma_{op} \tau_p)^{1/2} - \Gamma_{op} \tau_p; \quad \Gamma_{op} \tau_p < g_R x, \quad (27)$$

where  $x$  is the interaction length.

The interaction length ( $x$ ) becomes very small for backward scattering because the Stokes pulse and the laser pulse travel in opposite directions and hence, their overlap region cannot exceed the length of the laser pulse; viz., for a typical pico-second pulse laser, the interaction length is of the order of a millimeter. Thus following Wang [25], for very short durations ( $\tau_p \leq 10^{-10}$  s) the interaction length should be replaced by  $c_1 \tau_p / 2$  (where  $c_1$  is the velocity of light in the crystal medium). Consequently by making  $g_{TR} = 0$  in Eq. (27), the threshold-pump intensity for the onset of transient SRS can be obtained as:

$$I_{th} = \Gamma_{op} / 2G_R c_1, \quad (28)$$



where  $G_R = g_R / I_p$  is the steady state Raman gain coefficient per unit pump intensity, and  $I_p = 0.5\eta\epsilon_0 c_0 \left| \vec{E}_0 \right|^2$ . Using  $\Gamma_{op} = 3.7 \times 10^{11} \text{ s}^{-1}$  and  $g_R = 120 \text{ m}^{-1}$  at  $I_p = 3.55 \times 10^8 \text{ Wm}^{-2}$  for a centrosymmetric semiconductor-plasma and Eq. (27), we obtained the threshold value of pump intensity for the onset of Raman instability as  $2 \times 10^6 \text{ Wm}^{-2}$ . However, for comparatively long pulse duration ( $\tau_p \geq 10^{-9} \text{ s}$ ), the cell length can be taken equal to  $x$ , and under such circumstances, we obtain

$$g_{TR} = (\Gamma_{op} \tau_p)^{1/2} [-(\Gamma_{op} \tau_p)^{1/2} + (g_R x)^{1/2}]. \quad (29)$$

Using the above Eq., one may obtain the optimum value of pulse duration  $\tau_{p,opt}$ , above which no transient gain could be achieved. This can be obtained by making  $g_{TR} = 0$ , which yields:

$$\tau_{p,opt} \approx g_R / \Gamma_{op}. \quad (30)$$

A calculation for centrosymmetric semiconductor plasma using the values given earlier gives  $\tau_{p,opt} = 1.35 \times 10^{-6} \text{ s}$ . This value of  $\tau_{p,opt}$  not only explains the washing out of Raman gain at large pulse duration but also suggests that optimum pulse duration can be increased by increasing the intensity of the pump.

## RESULTS AND DISCUSSION

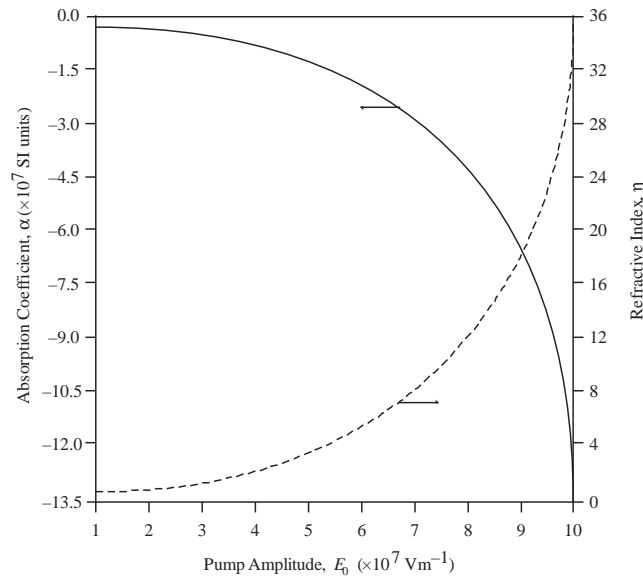
By analyzing Eq. (19), it can be realized that the external magnetic field and wave number have strong influence on  $\chi_{eff}^{(3)}$ . Considering the factors  $\delta_1^2$  and  $\delta_2^2$ , it may be concluded that  $\chi_{eff}^{(3)}$  is strongly influenced by carrier number density and diffusion coefficient. A close look at Eq. (19) reveals that the effective Raman susceptibility  $\chi_{eff}^{(3)}$  is a sensitive function of carrier concentration (via plasma frequency  $\omega_p$ ), externally applied static magnetic field (via cyclotron frequency  $\omega_c$ ) and diffusion coefficient (through the factors  $\delta_1$  and  $\delta_2$ ).  $\chi_{eff}^{(3)}$  with carrier density  $10^{24} \text{ m}^{-3}$  purely due to diffusion current is found to be  $\approx 2.55 \times 10^{-18} \text{ esu}$ . At lower concentration  $\chi_{eff}^{(3)}$  decreases by about five orders of magnitude and becomes potentially non-usable for the fabrication of cubic nonlinear devices. The magnitude of  $\chi_{eff}^{(3)}$  due to total current density (conduction as well as diffusion) agrees reasonably with the experimentally observed [26] and theoretically quoted values [21] using conduction current only.

A detailed numerical analysis of nonlinear absorption and refractive index of Raman scattered mode is made in a diffusive III-V semiconductor crystal, viz. n-InSb at 77 K. The crystal is assumed to be subjected to a  $10.6 \mu\text{m}$   $\text{CO}_2$  laser. The material constants are taken as:  $m = 0.0145m_e$  ( $m_e$  the free mass of electron),  $n_e = 10^{22} - 10^{24} \text{ m}^{-3}$ ,  $\omega_c = 0.1 - 0.9\omega_0$ ,  $\epsilon_\infty = 15.68$ ,  $\nu = 3.5 \times 10^{11} \text{ s}^{-1}$ ,  $N = 1.48 \times 10^{28} \text{ m}^{-3}$ ,  $\Gamma_{op} = 3.7 \times 10^{11} \text{ s}^{-1}$ ,  $\omega_{op} = 3.64 \times 10^{13} \text{ s}^{-1}$ ,  $(\partial\alpha / \partial u)_0 = 1.68 \times 10^{-16} \text{ mks units}$ .

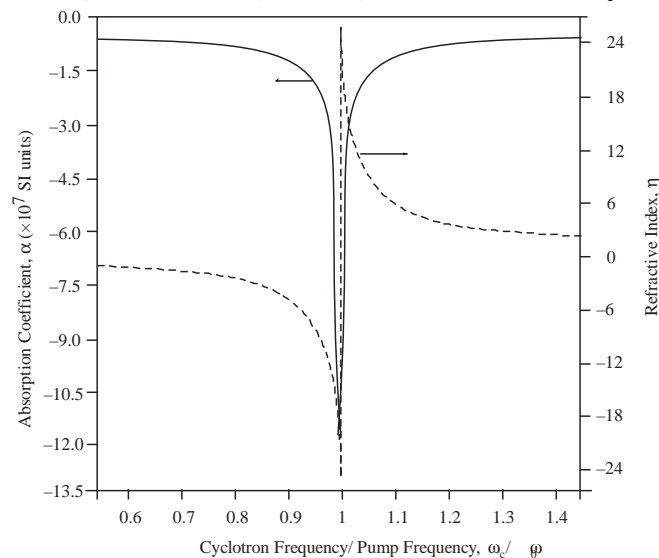
Let us now focus our attention on the physical parameters that affect the nonlinear absorption coefficient and refractive index of Raman scattered mode.

Fig. 2 shows the variation of absorption coefficient  $\alpha$  and refractive index  $\eta$  of Raman scattered mode with pump amplitude  $E_0$ . The curve reveals that with an increase in  $E_0$ ,  $\eta$  increases while  $\alpha$  decreases. The result is quite obvious because with increase in the transmitted power, absorption should decrease.





**Fig. 2. Variation of  $r$  and  $y$  of Raman scattered mode with pump amplitude  $E_0$  for  $\tilde{S}_c = 0.91\tilde{S}_0$ ,  $\tilde{S}_p = 0.12\tilde{S}_0$ ,  $D = 0.2 \text{ m}^2\text{s}^{-1}$ ,  $\theta = 60^\circ$ ,  $\psi = 135^\circ$  in InSb crystal.**



**Fig. 3. Variation of  $r$  (solid curve) and  $y$  (dotted curve) of Raman scattered mode as a function of magnetic field (via  $\tilde{S}_c / \tilde{S}_0$ ) for  $E_0 = 5 \times 10^7 \text{ Vm}^{-1}$ ,  $\tilde{S}_p = 0.12\tilde{S}_0$ ,  $D = 0.2 \text{ m}^2\text{s}^{-1}$ ,  $\theta = 60^\circ$ ,  $\psi = 135^\circ$  in InSb crystal.**

Fig. 3 represents the qualitative behaviour of absorption coefficient  $\alpha$  (solid curve) and refractive index  $\eta$  (dotted curve) of Raman scattered mode as a function of magnetic field (via  $\omega_c / \omega_0$ ). It is found that with increase in cyclotron frequency  $\omega_c$ ,  $\alpha$  decreases sharply and attains a minimum value of about  $-1.2 \times 10^8 \text{ m}^{-1}$  when  $\omega_c \sim \omega_0$ . With further increase in  $\omega_c$ ,  $\alpha$  increases. The magnetic field corresponding to  $\omega_c \sim \omega_0$  is 14.2 T. The refractive index  $\eta$  is a negative quantity for  $\omega_c < \omega_0$  and decreases with increasing  $\omega_c$ . A slight increase in tuning between  $\omega_c$  and  $\omega_0$  beyond this point causes a sharp rise in  $\eta$  making it vanish when  $\omega_c$  is closely tuned with  $\omega_0$ . After the resonance condition,  $\eta$  increases very sharply. With further increase in value of  $\omega_c$ ,  $\eta$  decreases rapidly and saturates at larger values of  $\omega_c$ . Such type of

variation is caused due to the term  $(\omega_0^2 - \omega_{cz}^2)$  in the denominator of third-order susceptibility (Eq. (19)). This type of behaviour of  $\eta$  may be utilized in the construction of optical switches.

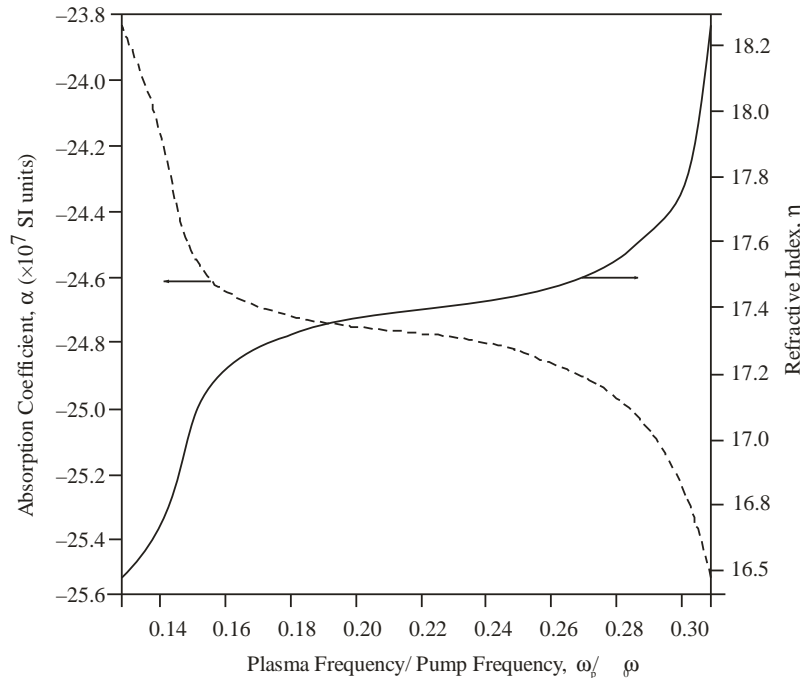


**Fig. 4. Variation of  $\alpha$  (solid curve) and  $\eta$  (dotted curve) of Raman scattered mode as a function of doping concentration (via  $\tilde{S}_p/\tilde{S}_0$ ) for  $E_0 = 5 \times 10^7 \text{ Vm}^{-1}$ ,  $\tilde{S}_c = 0.9\tilde{S}_0$ ,  $D = 0.2 \text{ m}^2\text{s}^{-1}$ ,  $\theta = 60^\circ$ ,  $\omega = 135^\circ$  in InSb crystal.**

Fig. 4 shows the variation of absorption coefficient  $\alpha$  (solid curve) and refractive index  $\eta$  (dotted curve) of Raman scattered mode as a function of doping concentration (via  $\omega_p/\omega_0$ ). Here again  $\alpha$  decreases while  $\eta$  increases with the increment in  $\omega_p$ . It may be inferred that a very slow rate of change is observed with both parameters in the regime  $0.16 \leq (\omega_p/\omega_0) \leq 0.28$ . Below and above these regime rates of change are quite fast. This type of variation can be understood from the fact that the nonlinear parameters for the Raman mode depend upon two factors: first the coupling of the electron motion with the acoustic mode responsible for induced current density and second the nonlinear force due to electrostriction responsible for deriving the absorption characteristics. The contribution of coupling between electron motion and the acoustic wave to  $\chi_{eff}^{(3)}$  can be seen through the term  $(\delta_1^2 - i\nu\omega_1)(\delta_2^2 + i\nu\omega_{op})$  inside the square bracket in Eq. (19). For  $\omega_p/\omega_0 < 0.16$ , this coupling parameter increases rapidly while polarization due to electrostriction remains almost constant; thus  $\alpha$  decreases while  $\eta$  increases sharply due to the induced current density. In the heavily doped regime when  $\omega_p/\omega_0 > 0.28$ , polarization due to electrostriction dominates the process which again resulted in a sharp decrement in  $\alpha$  and increment in  $\eta$ . In the middle regime, both effects combine to give a slow rate of change.

Figs. 5(a) and 5(b) shows the variation of absorption coefficient  $\alpha$  and refractive index  $\eta$  of Raman scattered mode, respectively as a function of scattering angle  $\phi$  for three different values of diffusion coefficient  $D$ .

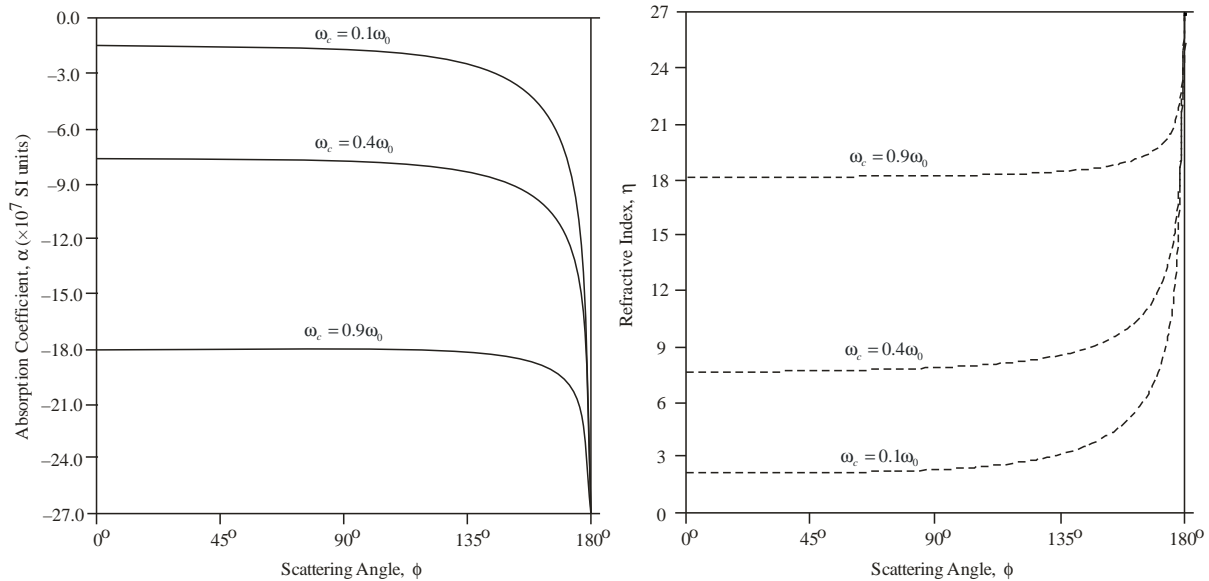


**Fig. 5. Variation of  $\alpha$  (first figure) and  $\eta$  (second figure) of Raman scattered mode as a function of scattering angle  $\phi$  for three different values of  $\tilde{S}_c$  in n-InSb crystal. Here  $E_0 = 5 \times 10^7 \text{ Vm}^{-1}$ ,  $\tilde{S}_c = 0.9\tilde{S}_0$ ,  $\tilde{S}_p = 0.12\tilde{S}_0$ ,  $D = 0.2 \text{ m}^2\text{s}^{-1}$  and  $\omega = 60^\circ$ .**

In all the three cases,  $\alpha$  starts with a relatively small (negative) value at  $\phi = 0^\circ$ , remains constant up to  $\phi = 135^\circ$ , and thereafter decreases sharply with increasing  $\phi$ . For backscattering ( $\phi = 180^\circ$ ),  $\alpha$  becomes independent of  $\omega_c$  and the curves coincide. On the other hand, in all the three cases,  $\eta$  starts with a relatively small value at  $\phi = 0^\circ$ , remains constant up to  $\phi = 135^\circ$ , and thereafter increases sharply with increasing  $\phi$ . For backscattering ( $\phi = 180^\circ$ ),  $\eta$  becomes independent of  $\omega_c$  and the curves coincide.

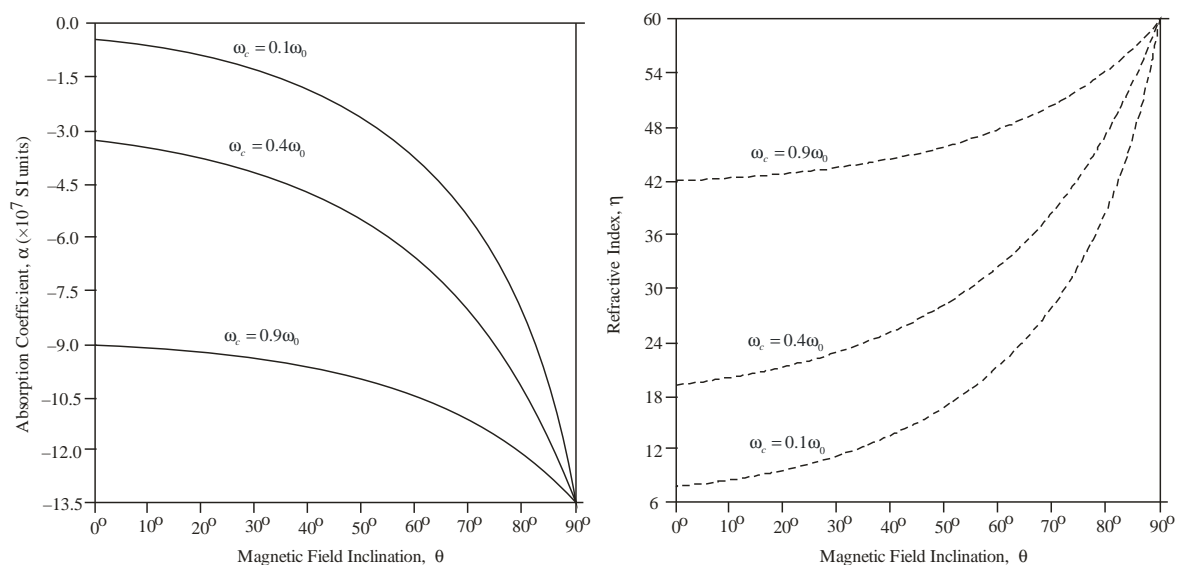


**Fig. 6. Variation of  $\alpha$  (first figure) and  $\eta$  (second figure) of Raman scattered mode as a function of  $\theta$  for three different values of  $\tilde{S}_c$  in n-InSb crystal. Here  $E_0 = 5 \times 10^7 \text{ Vm}^{-1}$ ,  $\tilde{S}_p = 0.12\tilde{S}_0$ ,  $D = 0.2 \text{ m}^2\text{s}^{-1}$  and  $\omega = 135^\circ$ .**

Figs. 6(a) and 6(b) shows the variation of absorption coefficient  $\alpha$  and refractive index  $\eta$  of Raman scattered mode, respectively as a function of inclination of the magnetic field with respect to the direction of

propagation  $\theta$  for three different values of  $\omega_c$  in n-InSb crystal. In all the three cases,  $\alpha$  starts with a relatively small (negative) value at  $\theta = 0^\circ$ , decreases continuously with increasing  $\theta$ . Initially, the curves start separately but come closer as  $\theta$  increases. For  $\theta = 90^\circ$ , when the contribution of magnetic Lorentz force becomes maximum,  $\alpha$  becomes independent of  $\theta$  and the curves coincide. On the other hand, in all the three cases,  $\eta$  starts with a relatively small value at  $\theta = 0^\circ$ , increases continuously with increasing  $\theta$ . Initially, the curves start separately but come closer as  $\theta$  increases. For  $\theta = 90^\circ$ , when the contribution of magnetic Lorentz force becomes maximum,  $\alpha$  becomes independent of  $\theta$  and the curves coincide.

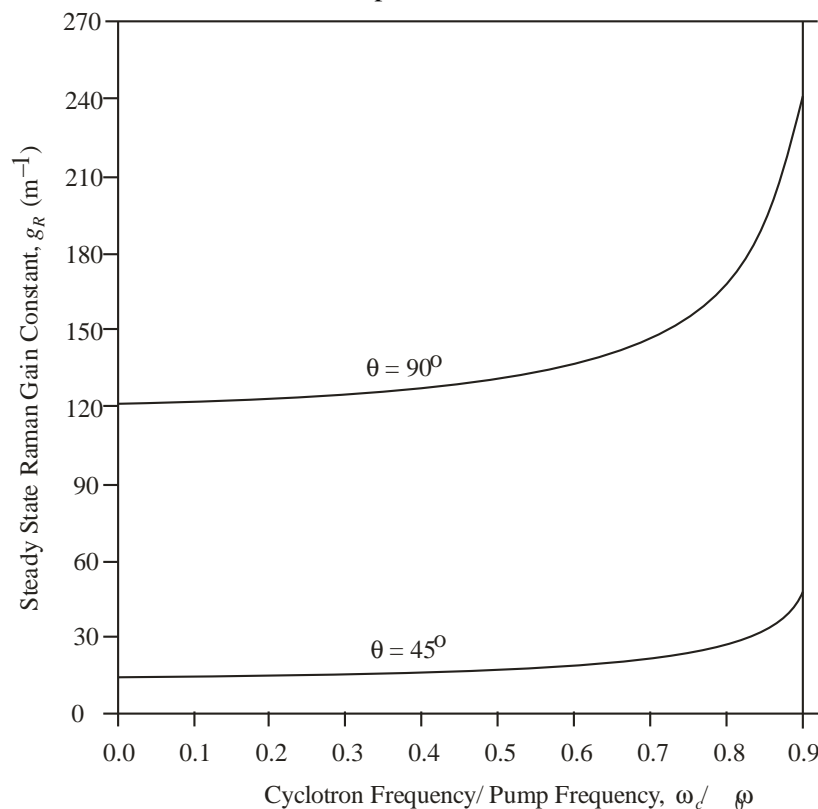


**Fig. 7. Variation of  $g_R$  as a function of  $B_0$  (via  $\tilde{\omega}_c/\tilde{\omega}_0$ ) for  $\theta = 45^\circ$  and  $90^\circ$  in n-InSb crystal. Here  $E_0 = 5 \times 10^7 \text{ Vm}^{-1}$ ,  $\tilde{S}_p = 0.12\tilde{S}_0$ ,  $D = 0.2 \text{ m}^2\text{s}^{-1}$  and  $\omega = 135^\circ$ .**

Fig. 7 shows the variation of steady-state Raman gain constant  $g_R$  as a function of externally applied static magnetic field (via  $\omega_c/\omega_0$ ) for  $\theta = 45^\circ$  and  $90^\circ$  in n-InSb crystal. In both the cases,  $g_R$  starts with a relatively lower value and is nearly independent of feeble magnetic fields (i.e. in the imposed cyclotron frequency regime  $\omega_c \leq 0.7\omega_0$ ). However,  $g_R$  increases very rapidly for cyclotron frequencies  $\omega_c > 0.7\omega_0$ . The externally applied magnetic field in transverse direction enhances  $g_R$  nearly three times than applied at an angle  $\theta = 45^\circ$  with the direction of propagation of pump beam.

Fig. 8 shows the variation of transient Raman constant  $g_{TR}$  with pump pulse duration  $\tau_p$  for two different values of externally applied static magnetic field ( $\omega_c = 0.2\omega_0$  and  $\omega_c = 0.9\omega_0$ ) in n-InSb crystal.

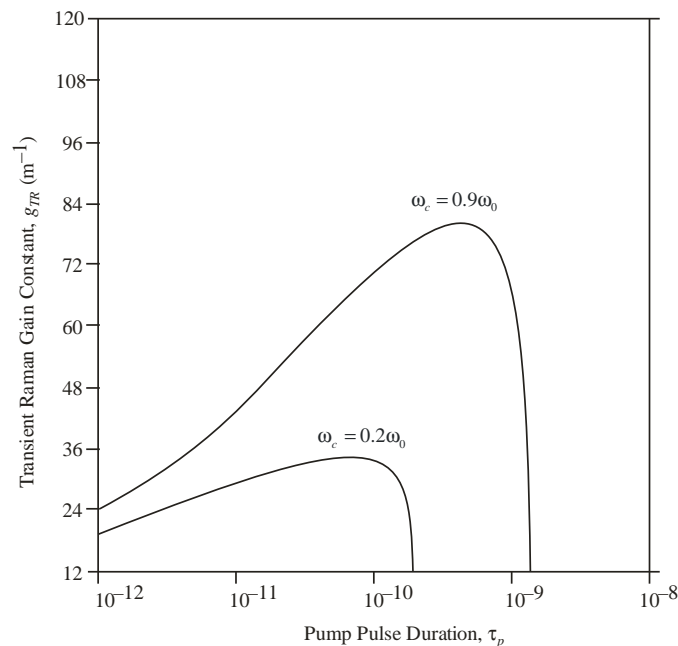


**Fig. 8. Variation of  $g_{TR}$  with  $\tau_p$  for  $\tilde{S}_c = 0.2\tilde{S}_0$  and  $\tilde{S}_c = 0.9\tilde{S}_0$  in n-InSb crystal. Here  $E_0 = 5 \times 10^7 \text{ Vm}^{-1}$ ,  $\tilde{S}_p = 0.12\tilde{S}_0$ ,  $D = 0.2 \text{ m}^2\text{s}^{-1}$  and  $W = 180^\circ$ .**

For a particular value of  $\omega_c$ ,  $g_{TR}$  increases with  $\tau_p$  and at a certain value of  $\tau_p$ ,  $g_{TR}$  attains a maximum value which remains constant for a certain range of  $\tau_p$ . Such regions can be regarded as quasi-steady states or quasi-saturation regimes. An increase in value of  $\omega_c$  shifts the gain saturation regime towards higher value of  $\tau_p$ . If  $\tau_p$  is chosen beyond quasi-saturation regime, the transient gain coefficient diminishes very rapidly.

## REFERENCES

- [1] Sutherlands R.L., 2003 "Handbook of Nonlinear Optics", Dekker: New York.
- [2] Brueckner K.A., Jorna S., 1974 "Laser-driven fusion", Rev. Mods. Phys. **46**, 325-367.
- [3] Liu C.S., Rosenbluth M.N., White R.B., 1974 "Raman and Brillouin scattering of electromagnetic waves in inhomogeneous plasmas", Phys. Fluids **17**, 1211-1219.
- [4] Woodburg E.J. and Ng W.K., 1962 "Ruby laser operation near the IR" Proc IRE **50**, 2347-2348.
- [5] Hellwarth R.W., 1963 "Theory of stimulated Raman scattering" Phys. Rev. **130**, 1850-1855.
- [6] Sodha M.S., Sharma R.P., Kaushik S.C., 1976 "Interaction of intense laser beams with plasma waves: stimulated Raman scattering", J. Appl. Phys. **47**, 3518-3523.
- [7] Maraghechi B., Willett J.E., 1978 "Raman backscattering of electromagnetic extraordinary waves in a magnetized inhomogeneous plasma", J. Plasma Phys. **20**, 859-865.
- [8] Maraghechi B., Willett J.E., 1979 "Raman backscattering of circularly polarized electromagnetic waves propagating along a magnetic field", J. Plasma Phys. **21**, 163-172.
- [9] Gibbs H.N., 1985 "Optical Bistability: Controlling Light with Light" (Academic: Orlando).
- [10] Wherrett B.S., 1989 "Optical Computing", Wherrett B.S., Tooley F.P.A. eds. (SUSSP: Edinburg) pp. 1-21.
- [11] Sen P.K., Apte N., Guha S., 1980 "Raman instability in n-type piezoelectric semiconductors", Phys. Rev. B **22**, 6340-6346.
- [12] Sen P., Sen P.K., 1985 "Theory of stimulated Raman and Brillouin scattering in noncentrosymmetric crystals", Phys. Rev. B **31**, 1034-1040.
- [13] Sen P., Sen P.K., 1986 "Correlation and competition between stimulated Raman and Brillouin scattering processes", Phys. Rev. B **33**, 1427-1435.
- [14] Ghosh S., Dixit S., 1985 "Stimulated Raman scattering and Raman instability of an intense helicon wave in longitudinally magnetized n-type piezoelectric semiconducting plasma, Phys. Stat. Sol. (b) **131**, 255-265.

- 
- [15] Singh M., Aghamkar P., Kishore N., Sen P.K., Perrone M.R., 2007 “Stimulated Raman scattering in weakly polar transversely magnetized doped semiconductors” *Phys. Rev. B* **76**, 012302-05.
  - [16] Neogi A., 1995 “Acousto-optic modulation in diffusive semiconductors”, *J. Appl. Phys.* **77**, 327-333.
  - [17] Ghosh S., Sharma G., Rishi M.P., 2003 “Parametric amplification in magnetized diffusive semiconductor plasmas”, *Physica B* **328**, 255-263.
  - [18] Ghosh S., Yadav N., 2007 “Stimulated Brillouin scattering in magnetized diffusive semiconductor plasmas”, *Eur. Phys. J. B* **59**, 173-178.
  - [19] Nimje N., Dubey S., Ghosh S.K., 2010 “Diffusion-induced modulation instability in magnetised semiconductor plasmas: effect of carrier heating”, *Eur. Phys. J. D*, **59**, 223-231.
  - [20] Nimje N., Dubey S., Ghosh S., 2012 “Amplitude modulation and demodulation of electromagnetic wave in magnetised acousto-optic diffusive semiconductor plasmas: Hot carrier effects”, *Opt. Laser Tech.* **44**, 744-748.
  - [21] Singh V. Pal, Singh M., 2016 “Stimulated Raman scattering in weakly polar narrow band gap magnetized semiconductors in the presence of hot carriers” *Opt. Quantum Electron.* **48**, 479-490.
  - [22] Yariv A., 1997 “Optical Electronics in Modern Communications”, University Press: Oxford, p. 479.
  - [23] Hopf F.A., Stegeman G.I., 1986 “Applied Classical Electrodynamics”, Wiley: New York, vol. 2, pp. 100-103.
  - [24] Carman R.L., Shimizu F., Wang C.S. Bloembergen N., 1970 “Theory of Stokes pulse shapes in transient stimulated Raman scattering”, *Phys. Rev. A* **2**, 60-72.
  - [25] Wang C.H., 1975 “Quantum Electronics”, Rabin H., Tang C.L. (Eds.), vol. 1, part A (Academic Press: New York), pp. 455-472.
  - [26] Muravjov A.V., Shastin V.N., 1991 “Landau Quantization and hot hole stimulated FIR emission in crossed electric and magnetic fields” *Opt. Quantum Electron.* **23**, S313-S321.